

# Speed control of hybrid energy sources fed BLDC motor drive with FOPID controller using various optimization techniques

Sushita Kanagaraj, Shanmugasundaram Nithaiyan

Department of Electrical and Electronics Engineering, Vels Institute of Science, Technology, and Advanced Studies, Chennai, India

## Article Info

### Article history:

Received May 19, 2022

Revised Aug 18, 2022

Accepted Sep 6, 2022

### Keywords:

BLDC motor  
FOPID  
MOA  
REHPS  
SEPIC converter

## ABSTRACT

This article suggests the control of current and speed approach to reduce the torque ripple in BLDC motor. Initially, the renewable energy hybrid power system (REHPS) is composed of a generation system of PV, fuel cell (FC), and the storage system of battery bank. This REHPS uses solar power as their main source of electricity during the day. It uses the fuel cell as a secondary source for maintenance at night or during periods of shaded conditions. The novelty of the proposed method is to achieve torque ripple minimization and to control the speed of the BLDC motor. The speed and error torque of the BLDC motor is optimized by mayfly optimization algorithm (MOA). The MOA provides gain parameters of the fractional order proportional–integral–derivative (FOPID) controller. The advantage of the proposed method is to improve the level of dependability and provide flexibility in solving the system error. The proposed model is implemented in MATLAB/Simulink and experimental setup. The results of the proposed method are compared with the existing research techniques such as particle swarm optimization (PSO) and moth flame algorithm (MFA).

*This is an open access article under the [CC BY-SA](https://creativecommons.org/licenses/by-sa/4.0/) license.*



## Corresponding Author:

Sushita Kanagaraj

Department of Electrical and Electronics Engineering

Vels Institute of Science, Technology and Advanced Studies

PV Vaithiyalingam Rd, Velan Nagar, Krishnapuram, Pallavaram, Chennai, Tamil Nadu 600117, India

Email: sushita.se@velsuniv.ac.in

## 1. INTRODUCTION

Because of fast populace development and expanding interest for energy, the pattern is towards new and sustainable power sources, for example, sun oriented, wind, and hydrogen. It explores the reasons for a procedure that utilizes sustainable power sources, for example, sun-oriented force and wind ability to create power and hydrogen. A BLDC drive is characterized as a sort of self-simultaneous rotating motor constrained by an electronic suburbanite instead of DC motors with a mechanical commutator [1], [2]. So, brushless direct current (BLDC) motors don't have brushes, however DC motors had brushes. Because BLDC motors are brushless, their life can be increased and maintenance operations avoided. The construction of the BLDC motor is like a permanent magnet synchronous motor (PMSM) [3]-[6]. Three phase induction motor runs with newly developed power cable model and analysis the cable behavior [7], [8]. Accordingly, in this study proposed renewable energy sources which includes PV, battery, and proton exchange membrane fuel cell (PEMFC) power supply are used as power supply for BLDC motor. In order to enhance the pulse width modulation (PWM) method, the metaheuristic methods are the most recent advancement [9], [10].

## 2. PROPOSED METHOD

Figure 1 shows the control structure of BLDC motor for speed and torque regulation. The hybrid renewable energy which includes PV, FC, and energy storage system is used as an input supply for the proposed system. The speed regulation is equipped with the speed controller (fractional order proportional–integral–derivative (FOPID) based mayfly optimization algorithm (MOA)) to evaluate the reference BLDC motor speed in accordance with speed error. On the basis of distortion error, the optimal gain tuning controller (FOPID based MOA) is designed and their corresponding control signals are determined. The modified single-ended primary-inductor converter (SEPIC) converter is used to achieve torque ripple reduction with high efficiency and good regulation under different load conditions.

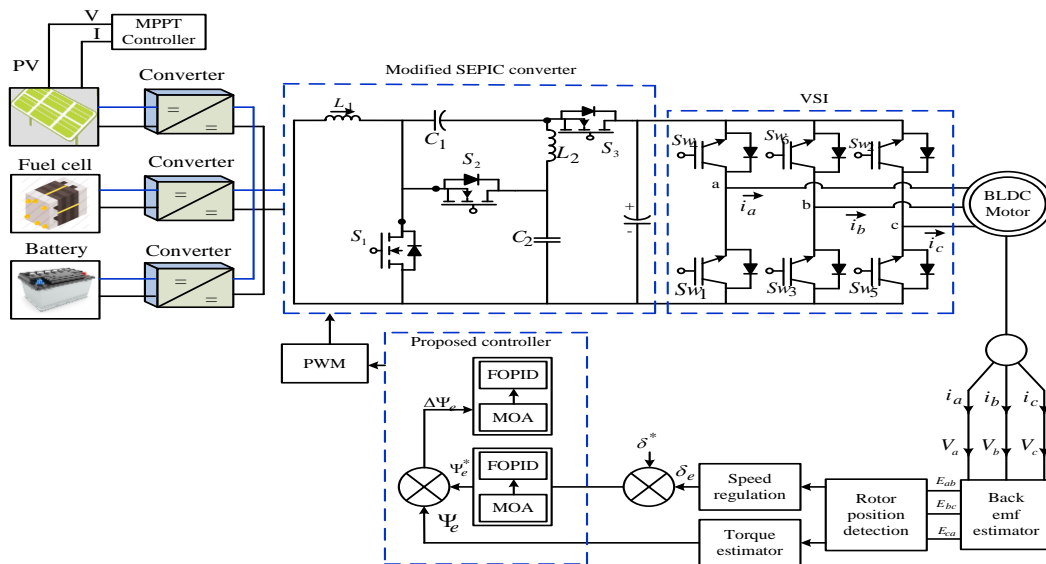


Figure 1. Proposed control structure of BLDC motor drive

### 2.1. Photovoltaic systems

Photovoltaic systems (PVS) convert light energy into electricity to generate electricity. The diode model consists of a power supply; a parallel diode with two resistors is to represent each photovoltaic (PV) panel. In PVS, a DC/DC converter is included in the maximum power point tracker (MPPT) controller. MPPT controllers are used to achieve maximum performance under normal radiation conditions [11]-[13]. PV system's output performance depends on solar irradiation and temperature. MPPT is the most effective solution to extract the maximum power from the PV system [14]. The MPPT controller activates the duty cycle of the frequency converter to increase the MPP voltage (minimum power point) [15].

### 2.2. Fuel cell system

Renewable energy fuel cells use energy from energy sources; recommended for its advantages such as zero emission, higher energy power than wind, and other renewable energy systems [16]. Proton exchange membrane fuel cell (PEMFC) due to its unique properties and overall fuel economy proves to be a promising component of hybrid systems. PEMFC has a very low temperature with high power. The PMFC uses hydrogen to produce electricity in an electrochemical reaction using hydrogen and oxygen, where its only by-product is water, and therefore its emission.

### 2.3. Energy storage system

Storage systems are required for renewable energies because there is not enough PV to support the load. A rechargeable battery is used to store excess energy in chemical form. The purpose is that the energy demand meets the load requirement when no generating capacity is available. The battery life is calculated in the terms of state of charge (SOC).

### 2.4. Design of BLDC motor

The BLDC motor is electronically commutated DC motor with stator and rotor along rings that are around the stator posts and connected with fully inverted assemblies to frame the motor stages. The rotating

part of BLDC motor is rotor and the stationary part is stator [17]. The permanent magnets are fixed in the rotor and moves electromagnets to stator. The output voltage of the BLDC motor is described in (1)-(3).

$$A_V = A_R A_I + A_L(\theta, A_I) \frac{dA_I}{dt} + A_E \tag{1}$$

$$B_V = B_R B_I + B_L(\theta, B_I) \frac{dB_I}{dt} + B_E \tag{2}$$

$$C_V = C_R C_I + C_L(\theta, C_I) \frac{dC_I}{dt} + C_E \tag{3}$$

Where,  $ABC_V$  and  $ABC_I$  are the three-phase input voltages and BLDC variable speed drive currents. The resistances and inductances of the three phases are represented as  $ABC_R$  and  $ABC_L$ ,  $\theta$  represents the position of rotor angle and back electromagnetic fields (EMFs) of the BLDC motor is represented as  $ABC_E$ .

**2.5. Design of speed controller**

The speed controller design and demonstrate the exchanging capacity of a FOPID speed regulator which is communicated in (4).

$$G_S(s) = \Delta e_\delta(s) \times \left[ \Delta \check{K}_{p\delta} + \frac{\Delta \check{K}_{i\delta}}{s^{\lambda\delta}} + \Delta \check{K}_{d\delta} s^{\mu\delta} \right] \tag{4}$$

Where,  $G_S(s)$  is the FOPID output speed;  $\Delta e_\delta(s)$  is the speed error;  $\Delta \check{K}_{p\delta}$ ,  $\Delta \check{K}_{i\delta}$ ,  $\Delta \check{K}_{d\delta}$ ,  $\check{\lambda}$  and  $\check{\mu}$  are the parameters of FOPID controller.

**2.6. Design of current controller**

Each current control loop has a corresponding controller configuration which includes a FOPID current controller and a PWM controller. The switching function of an actual FOPID controller is generally expressed in parallel according to (5):

$$G_C(s) = \Delta e_i(s) \times \left[ \Delta \check{K}_{pc} + \frac{\Delta \check{K}_{ic}}{s^{\lambda c}} + \Delta \check{K}_{dc} s^{\mu c} \right] \tag{5}$$

where,  $G_C(s)$  is FOPID output current;  $\Delta e_i(s)$  is the current error;  $\Delta \check{K}_{pc}$ ,  $\Delta \check{K}_{is}$ ,  $\Delta \check{K}_{dc}$ ,  $\check{\lambda}$ , and  $\check{\mu}$  are the parameters of FOPID controller.

**2.7. Design of modified SEPIC converter**

The modified SEPIC converter design is type of DC-DC converter whose output voltage is greater than, less than, or equal to input. The output of modified SEPIC converter is controlled by the duty cycle of the transistor [18]. The SEPIC converter operates in two modes, mode I-continuous conduction mode (CCM) and mode II-discontinuous conduction mode (DCM) that is used to control the intermediate circuit voltage. The proposed SEPIC converter is the combination of three semiconductor switches ( $S_1$ ,  $S_2$ , and  $S_3$ ), two capacitors ( $C_1$ ,  $C_2$ ) and two inductors ( $L_1$ ,  $L_2$ ). Mode of operation:

- a. Mode I: Figure 2(a) shows mode I of an altered modified SEPIC converter fed to BLDC motor. The switch  $S_1$  is turned on and the switches  $S_2 - S_3$  are turned-off during this mode of operation. The inductors  $L_1$  and  $L_2$  store energy with the voltage  $V_1$  applied to the inductor  $L_1$  and the voltage  $V_{C2} - V_{C1} = V_2$  applied to the inductor  $L_2$ .
- b. Mode II: Figure 2(b) shows mode II of an altered modified SEPIC converter fed to BLDC motor. The switch  $S_1$  is off and the switches  $S_2 - S_3$  turned-on. During this phase, energy is transferred from inductors  $L_1$  and  $L_2$  to capacitors. The voltage applied to the inductors is  $-(V_{C2} - V_1) = (V_1 - V_{C2})$  for  $L_1$  and  $-(V_2 - V_{C2}) = (V_{C2} - V_2)$  for  $L_2$ .

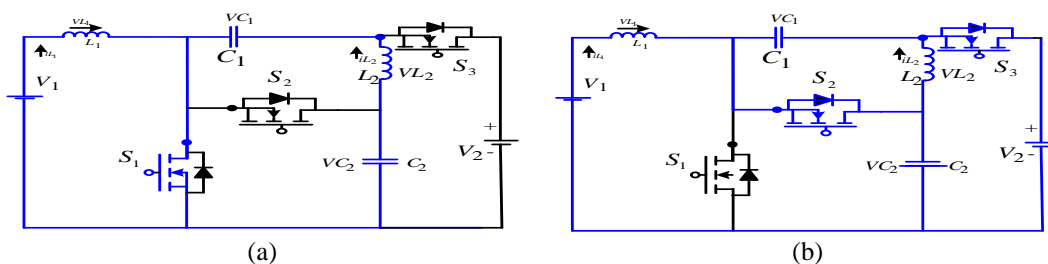


Figure 2. Operating modes of modified SEPIC converter (a) mode I and (b) mode II

### 3. PREDICTION OF GAIN PARAMETERS BASED ON PROPOSED MULTI-OBJECTIVE MOA ALGORITHM

The MOA is a hybrid algorithm of particle swarm organization and differential evolution algorithm. The hybrid optimization algorithm solves optimization problem. They are integrated to overcome the drawbacks of PSO and moth flame algorithm (MFA) [19]. Moth-flame optimization (MFO) algorithm is a nature inspired metaheuristic based movement of moths in the environment known which is known as transverse orientation [20], [21]. It is a metaheuristic optimization algorithm based on the flight behavior of adult mayflies, including hybrids, mutations, group gatherings, nuptial dances, and occasional walks [22], [23]. After hatching, an immature mayfly become visible to the naked eye and grows as aquatic nymphs for several years before they become adult. An adult fly only lives for a few days until it reaches its breeding goal. To attract women, most adult male gather in groups a few feet above the water and perform nuptial dance in the pattern of up and down [24], [25]. Female mayfly goes to these male to mate in air. This process may take a few seconds. The eggs are then thrown into the water and the cycle continues. In the proposed scheme, the implementation of the MOA algorithm leads to the optimization of control parameters in the BLDC motor drive system [26]-[28]. The initial values of  $K_p$ ,  $K_i$ , and  $K_d$  of the fractional order of differentiator and integrator terms are drawn from MFO algorithm [29].

#### Steps involved in multi-objective MOA

Step\_1: Objective function  $f(x)$  where  $x = (x_1, x_2, x_d) T$   
 Step\_2: Initialization of male may fly population  $x_k$  where  $k = 1, 2, \dots, N$  and velocities  $vm_k$ .  
 Step\_3: Initialization of female may fly population  $y_k$  where  $k = 1, 2, \dots, N$  and velocities  $vfk$ .  
 Step\_4: Evaluate the solutions of defined objective function.  
 Step\_5: Store the no dominated solutions found in exterior depository.  
 Step\_6: Sort the mayflies  
 Step\_7: Do while stopping if criteria are not met  
 Step\_8: Update position and velocities of male and female mayflies  
 Step\_9: Evaluate solutions  
 Step\_10: If a new mayfly dominates its personal best  
 Step\_11: Replace personal best with new solution  
 Step\_12: If none dominates the other  
 Step\_13: The new solution has 50% chance to replace personal best  
 Step\_13: Rank mayflies  
 Step\_14: Mate mayflies  
 Step\_15: Evaluate offspring  
 Step\_16: Categorize offspring randomly to male and female  
 Step\_17: If offspring dominates same gender parent  
 Step\_18: Replace parent with an offspring  
 Step\_19: Enter all the no dominated solutions found in exterior depository  
 Step\_20: Sort the no dominated solutions and replace the depository if needed  
 Step\_21: End while

### 4. RESULTS AND DISCUSSION

The proposed method helps in reducing the torque ripple of the BLDC motor with hybrid renewable energy storage system and its performance is analyzed and compared with existing methods. The proposed technique is carried out in MATLAB/Simulink (R2018a) platform and in the experimental setup. Here, speed and current control of the BLDC motor have been performed by the proposed optimized FOPID controller. The proposed FOPID controller using MOA optimization technique based on the multi-objective function controls the BLDC motor in the vehicle system. The effectiveness of the proposed control method is analyzed by comparing it with the conventional methods such as MFA and particle swarm optimization algorithm (PSO). Figure 3 shows the simulation of BLDC motor drive with renewable energy sources in MATLAB/Simulink.

#### 4.1. Performance analysis

The BLDC motor is tested under following two modes and the performance of the proposed controller is verified.

a. Mode I: the PV, fuel cell, and battery source is kept at constant and load is varied

The BLDC motor speed is controlled based on the motor input parameters such as EMF and current. The torque based on the input current and the back EMF is described in Figure 4(a) and Figure 4(b) respectively. The BLDC motor input current and the emf is varied up to timeframe of 0.5 seconds, after which the current and emf is constant.

Figures 5(a) to (c) shows the converter output, torque and speed of proposed methodology and existing methodology respectively. This comparison figure shows that the proposed method take less settling

time and torque ripple is reduced up to 4.75% compared to MFA and PSO algorithm whose torque ripples as 6.45% and 9.32% respectively.

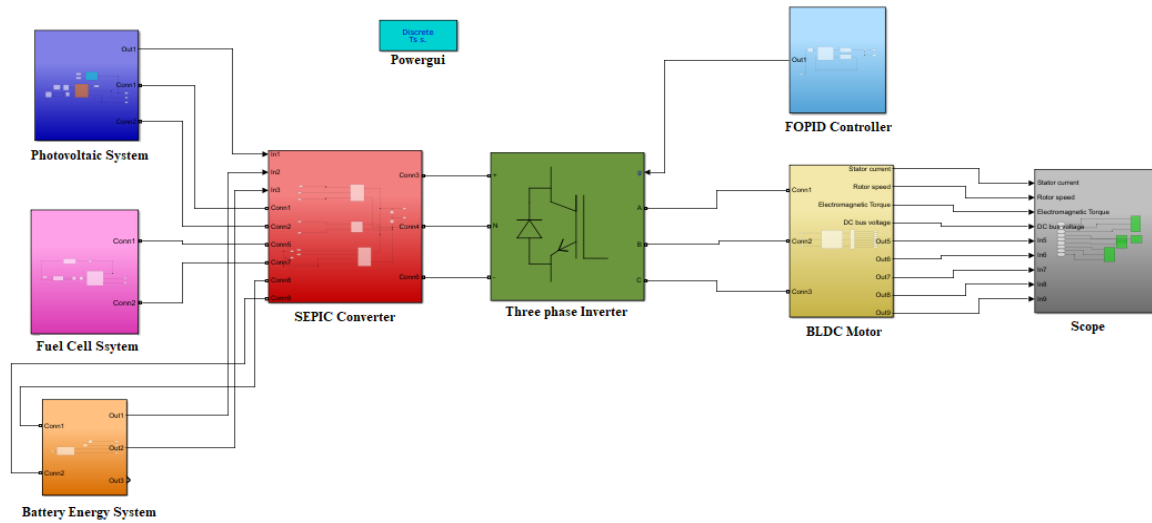


Figure 3. MATLAB/Simulink structure of BLDC motor drive with controller

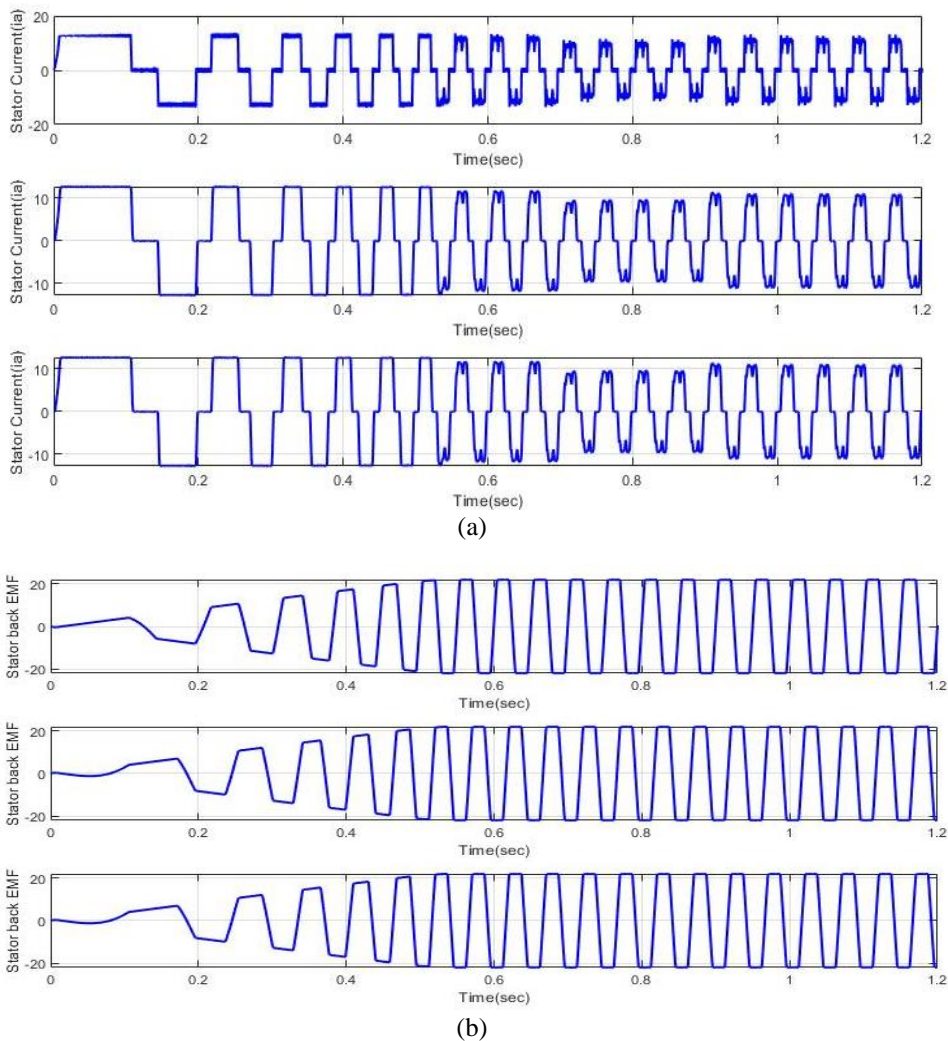


Figure 4. Output of parameters (a) stator current (ia, ib, ic) and (b) back EMF (ea, eb, ec) in mode I

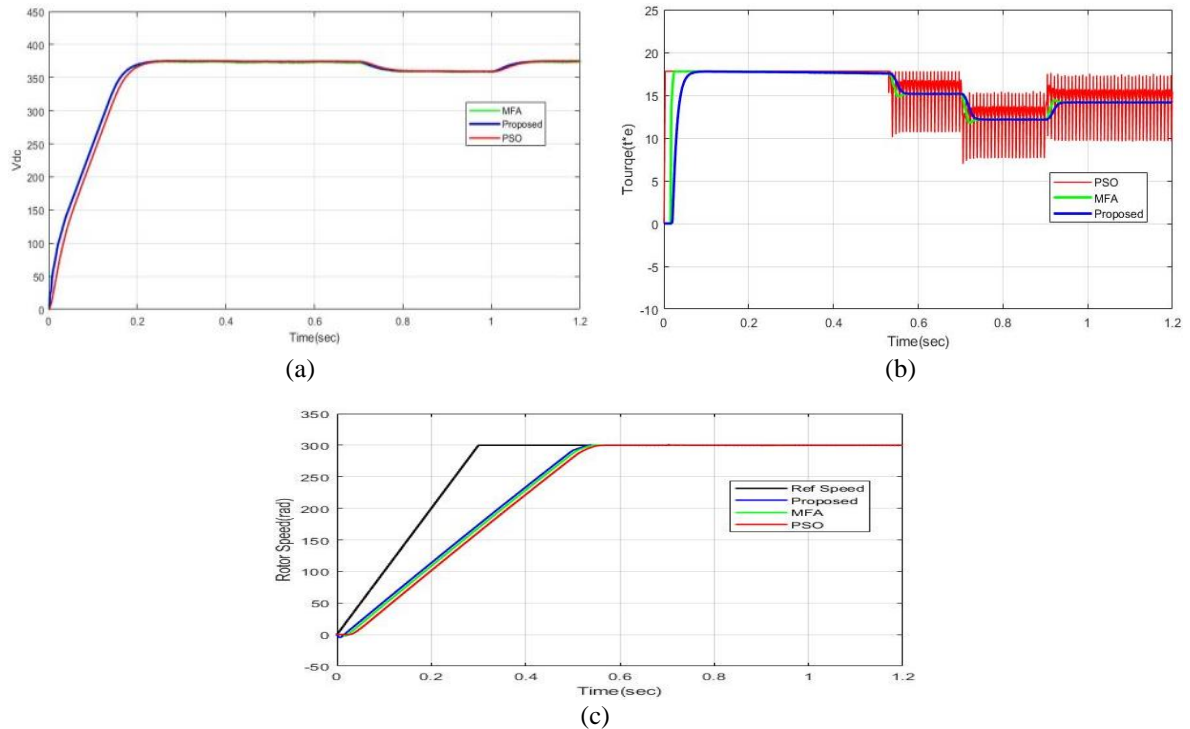


Figure 5. Comparative analysis of (a) converter output, (b) torque, and (c) speed of proposed and existing method–mode I

Figure 6 shows the energy generated by renewable energy sources. The maximum power of PVS is 10 KW. The output power of the FCS is 2KW and total required power output is 12KW at 0-1.2 seconds. Based on the result analysis, the proposed system meets the required demand.

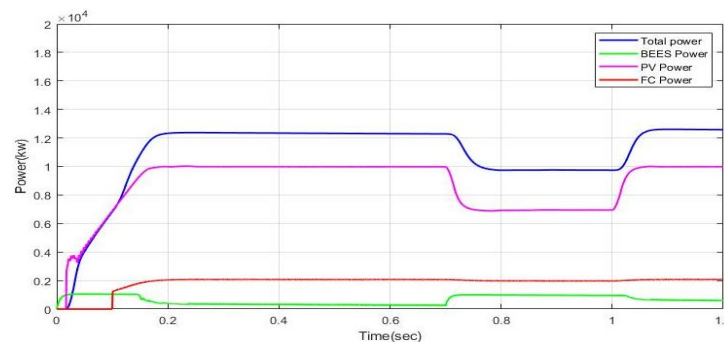


Figure 6. Comparative analysis of generated power in mode I

b. Mode II: the PV, fuel cell, and battery source is varied and load is kept constant

In this mode II analysis, the load is kept constant and renewable energy sources are varied. In Figure 7, the torque is estimated at 17 Nm and reference speed is 300 rad/s. Based on the speed of the motor, the input current and back determined in mode I. The converter output, speed and torque of the proposed BLDC motor with renewable energy source is evaluated and analyzed with existing techniques. Figure 7(a) shows the performance analysis of converter voltage. The comparative analysis of the torque with the existing methods is determined in Figure 7(b). In this waveform from time period 0.7 sec to 0.9 sec disturbances have occurred, after which the torque reaches reference torque and based on the oscillation the proposed MOA is better than the existing methods such as MFA and PSO. Figure 7(c) analyses the speed performance of the proposed method which is superior to that of the existing methods like MFA and PSO algorithm. The proposed method has rise time 0.025 sec, settling time 0.05 sec, and there is no peak overshoot. The MFA and PSO algorithm have the settling time as 0.525 sec and 0.538 sec respectively.

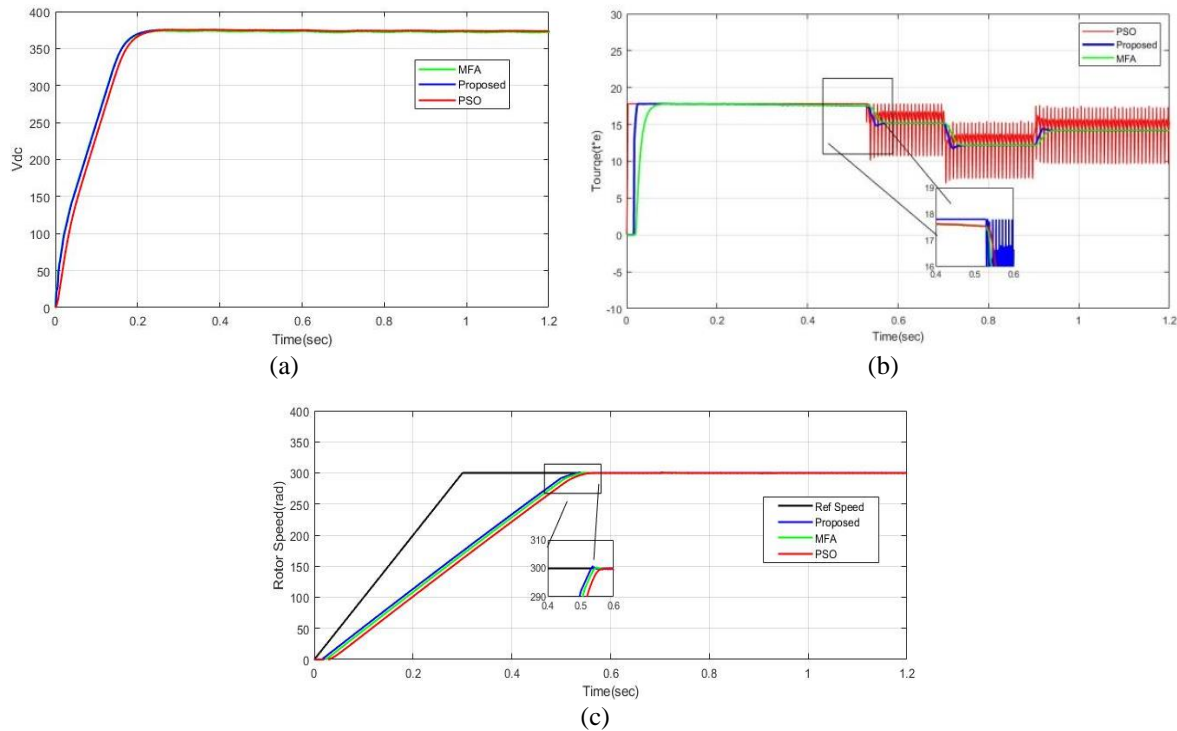


Figure 7. Comparative analysis of (a) converter output (b) torque, and (c) speed of proposed and existing method–mode II

Figure 8 shows the generated power of renewable energy hybrid power system. The load demand is met by the generated power of PVS, FCS and energy storage system with the help of the FOPID and MOA optimization technique. The total required demand is 12KW, the PV generated power is 10 KW and the fuel cell generated power is 2 KW. The energy storage system is charging at 0.3-0.6 sec. The required power demand is compensated with the PV, fuel cell system and energy storage system.

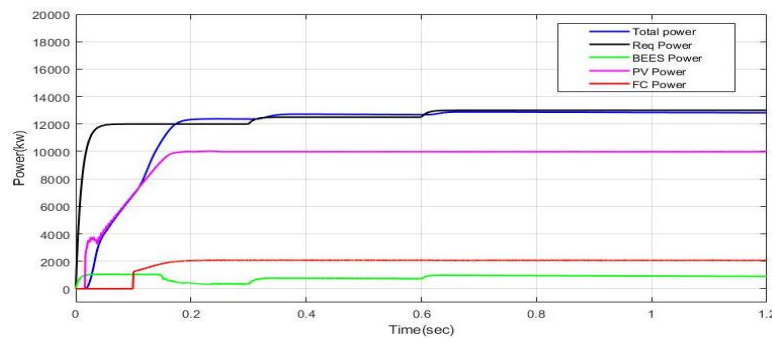


Figure 8. Comparative analysis of generated power in mode II

#### 4.2. Experimental results

This section presents the experimental results to establish the connections and to demonstrate the advantages of the BLDC-based PVC, FCS, and energy storage system based converter. The 3 KW PV test platform contains 24 PV modules. Each PV module has a maximum power of 121 W and a maximum power point voltage of 27 V (25 °C, 1000 W/m<sup>2</sup>) under standard voltage conditions. In this experimental setup, a BLDC motor based on renewable energy was designed based on solar radiation and ambient temperature profiles. Along with the PV, the system has integrated control between the fuel cell and the energy storage system. The experimental setup installation is shown in Figure 9. Figures 10(a) to (d) shows the converter output voltage, stator current, speed and torque of BLDC motor respectively. The experimental output of PV voltage, fuel cell voltage, and battery voltage in renewable energy sources is shown in Figures 11(a) to (c)

respectively. Thus, the experimental results also verify the effectiveness of the modified SEPIC converter based FOPID control strategy.

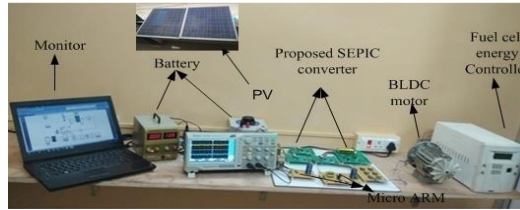


Figure 9. Experimental setup of BLDC motor drive system

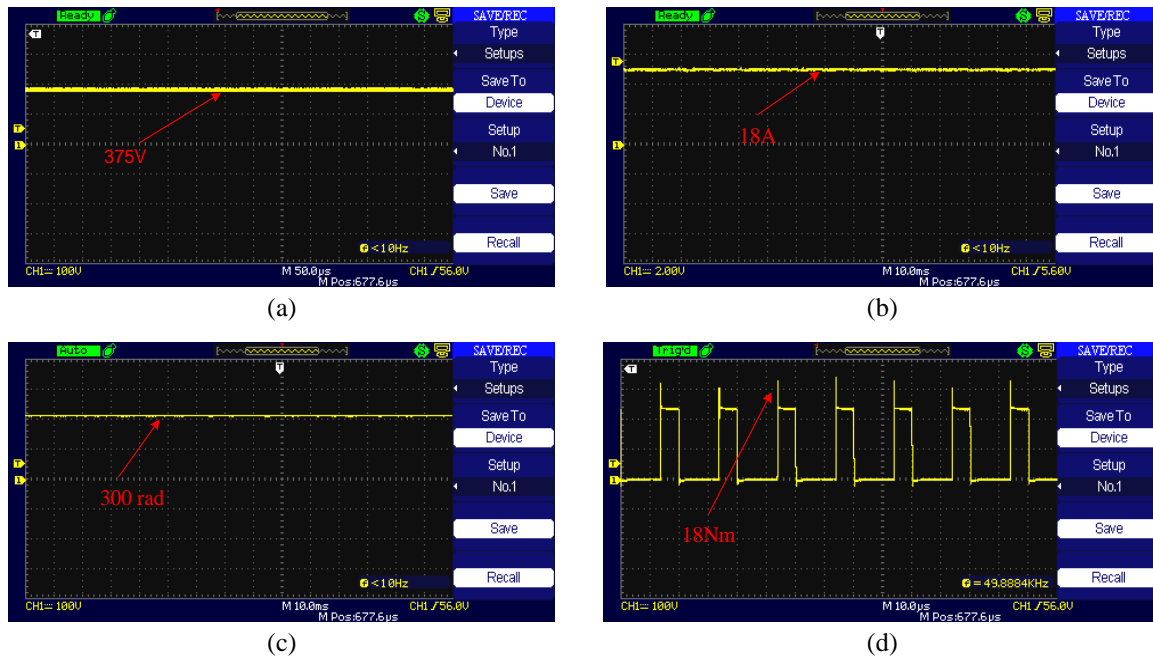


Figure 10. Experimental results of (a) converter output voltage (b) stator current (c) speed and (d) torque in BLDC motor drive

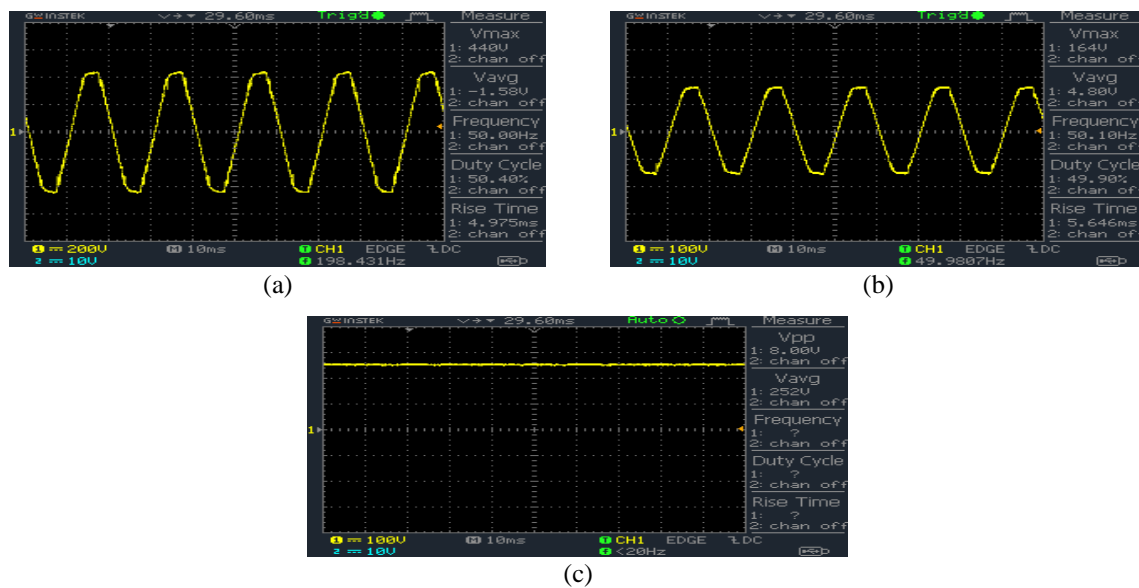


Figure 11. Experimental results of (a) PV voltage, (b) fuel cell voltage, and (c) battery voltage



## 5. CONCLUSION

This article presents a hybrid renewable energy source for a BLDC motor as a power source and proposes an advanced FOPID controller to control the BLDC motor speed and current. The proposed controller is based on the MOA approach and works on the MATLAB/Simulink platform and experimental setup. The proposed MOA is evaluated to optimize the improved gain parameters of the FOPID controller. The performance analysis of the proposed system parameters such as converter voltage, speed, current, and torque ripples is determined. From the achievable results, the proposed MOA with FOPID controller-based modified SEPIC converter provides the best solution for the BLDC motor with REHPS to reduce torque ripple and provides a better current profile compared to the existing methods. With optimal design parameters, the BLDC motor with REHPS achieves a torque of 4.75% which is a significant improvement over the existing methodologies.




## REFERENCES

- [1] M. Sigala, A. Beer, L. Hodgson, and A. O'Connor, "Big data for measuring the impact of tourism economic development programmes: a process and quality criteria framework for using big data," *Big Data and Innovation in Tourism, Travel, and Hospitality*, 2019, pp. 57–73, doi: 10.1007/978-981-13-6339-9\_4.
- [2] P. Karekar, C. Shrutika, S. Shadab, B. B. Pimple, and S. R. Wagh, "Real-time simulation for torque ripple minimization of BLDC motor using low pass compensator," *2020 International Conference on Electrical Machines (ICEM)*, 2020, pp. 1213-1218, doi: 10.1109/ICEM49940.2020.9270878.
- [3] A. G. de Castro, W. C. A. Pereira, T. E. P. de Almeida, C. M. R. de Oliveira, J. R. B. de A. Monteiro, and A. A. de Oliveira, "Improved finite control-set model-based direct power control of BLDC motor with reduced torque ripple," in *IEEE Transactions on Industry Applications*, vol. 54, no. 5, pp. 4476-4484, Sept.-Oct. 2018, doi: 10.1109/TIA.2018.2835394.
- [4] S. F. Toloue, S. H. Kamali, and M. Moallem, "Torque ripple minimization and control of a permanent magnet synchronous motor using multiobjective extremum seeking," in *IEEE/ASME Transactions on Mechatronics*, vol. 24, no. 5, pp. 2151-2160, Oct. 2019, doi: 10.1109/TMECH.2019.2929390.
- [5] R. Cui, Y. Fan and C. Li, "On-line inter-turn short-circuit fault diagnosis and torque ripple minimization control strategy based on OW five-phase BFTHE-IPM," in *IEEE Transactions on Energy Conversion*, vol. 33, no. 4, pp. 2200-2209, Dec. 2018, doi: 10.1109/TEC.2018.2851615.
- [6] C. K. Lad and R. Chudamani, "Simple overlap angle control strategy for commutation torque ripple minimization in BLDC motor drive," *IET Electric Power Applications*, vol. 12, no. 6, pp. 797-807, Mar. 2018, doi: 10.1049/iet-epa.2017.0644.
- [7] X. Yao, G. Lu, J. Zhao, and H. Lin, "Torque ripple minimization in brushless DC motor with optimal current vector control technique," *2018 Chinese Automation Congress (CAC)*, 2018, pp. 2524-2529, doi: 10.1109/CAC.2018.8623084.
- [8] N. Shanmugasundaram and S. Thangavel, "High frequency power cable modeling for screen voltage calculation of different cable length with induction motor drive system (VFD)," *ARPN Journal of Motorering and Applied Sciences*, vol. 10, no. 20, pp. 9150-9158, 2015.
- [9] N. Shanmugasundaram and S. Thangavel, "Modeling and simulation analysis of power cable a three level inverter fed induction motor drive," *Journal of Computational and Theoretical Nanoscience*, vol. 14, no. 2, pp. 972-978, Feb. 2017, doi: 10.1166/jctn.2017.6390.
- [10] M. H. Zafar, N. M. Khan, A. F. Mirza, and M. Mansoor, "Bio-inspired optimization algorithms based maximum power point tracking technique for photovoltaic systems under partial shading and complex partial shading conditions," *Sustainable Cities and Society*, vol. 76, p. 127279, Aug. 2021, doi: 10.1016/j.jclepro.2021.127279.
- [11] A. D. G. Jegha, M. S. P. S. Nallapaneni, M. Kumar, U. Subramaniam, and P. Sanjeevikumar, "A high gain DC-DC converter with grey wolf optimizer based MPPT algorithm for PV Fed BLDC motor drive," *Applied Sciences*, vol. 10, no. 8, p. 2797, Apr. 2020, doi: 10.3390/app10082797.
- [12] H. Abouadane, A. Fakkar, D. Sera, A. Lashab, S. Spataru, and T. Kerekes, "Multiple-power-sample based P&O MPPT for fast-changing irradiance conditions for a simple implementation," in *IEEE Journal of Photovoltaics*, vol. 10, no. 5, pp. 1481-1488, Sept. 2020, doi: 10.1109/JPHOTOV.2020.3009781.
- [13] Z. Alqaisi and Y. Mahmoud, "Comprehensive study of partially shaded PV modules with overlapping diodes," in *IEEE Access*, vol. 7, pp. 172665-172675, 2019, doi: 10.1109/ACCESS.2019.2956916.
- [14] M. Alsumiri, "Residual incremental conductance based nonparametric MPPT control for solar photovoltaic energy conversion system," in *IEEE Access*, vol. 7, pp. 87901-87906, 2019, doi: 10.1109/ACCESS.2019.2925687.
- [15] M. H. Anowar and P. Roy, "A modified incremental conductance based photovoltaic MPPT charge controller," *2019 International Conference on Electrical, Computer and Communication Engineering (ECCE)*, 2019, pp. 1-5, doi: 10.1109/ECACE.2019.8679308.
- [16] W. Hayder, E. Ogluari, A. Dolara, A. Abid, M. B. Hamed, and L. Sbata, "Improved PSO: a comparative study in MPPT algorithm for PV system control under partial shading conditions," *Energies*, vol. 13, no. 8, p. 2035, Apr. 2020, doi: 10.3390/en13082035.
- [17] T. Yigit and H. Celik, "Speed controlling of the PEM fuel cell powered BLDC motor with FOPI optimized by MSA," *International Journal of Hydrogen Energy*, vol. 45, no. 60, pp. 35097-35107, Dec. 2020, doi: 10.1016/j.ijhydene.2020.04.091.
- [18] D. Pallav and K. N. Santanu, "Grey wolf optimizer based PID controller for speed control of BLDC motor," *Journal of Electrical Engineering & Technology*, vol. 16, pp. 955-961, Jan. 2021, doi: 10.1007/s42835-021-00660-5.
- [19] S. Natchimuthu, M. Chinnusamy, and A. P. Mark, "Experimental investigation of PV based modified SEPIC converter fed hybrid electric vehicle (PV-HEV)," *International Journal of Circuit Theory and Applications*, vol. 48, no. 6, pp. 980-996, Feb. 2020, doi: 10.1002/cta.2766.
- [20] Z. Yang, K. Shi, A. Wu, M. Qiu, and Y. Hu, "A Hybrid method based on particle swarm optimization and moth-flame optimization," *2019 11th International Conference on Intelligent Human-Machine Systems and Cybernetics (IHMSC)*, 2019, pp. 207-210, doi: 10.1109/IHMSC.2019.10144.
- [21] Y. Xu *et al.*, "An efficient chaotic mutative moth-flame-inspired optimizer for global optimization tasks," *Expert Systems with Applications*, vol. 129, pp. 135-155, Sep. 2019, doi: 10.1016/j.eswa.2019.03.043.
- [22] M. Shehab, L. Abualigah, H. A. AlHamad, H. Alabool, M. Alshinwan, and A. M. Khasawneh, "Moth-flame optimization algorithm: variants and applications," *Neural Computing and Applications*, vol. 32, no. 11, pp. 9859-9884, Jul. 2020, doi: 10.1007/s00521-019-04570-6.




- [23] K. Zervoudakis and S. Tsafarakis, "A mayfly optimization algorithm," *Computers & Industrial Motorering*, vol. 145, p. 106559, Jul. 2020, doi: 10.1016/j.cie.2020.106559.
- [24] T. Bhattacharyya, B. Chatterjee, P. K. Singh, J. H. Yoon, Z. W. Geem, and R. Sarkar, "Mayfly in harmony: a new hybrid meta-heuristic feature selection algorithm," in *IEEE Access*, vol. 8, pp. 195929-195945, 2020, doi: 10.1109/ACCESS.2020.3031718.
- [25] Md. H. K. Roni, M. S. Rana, H. R. Pota, Md. M. Hasan, and M. S. Hussain, "Recent trends in bio-inspired meta-heuristic optimization techniques in control applications for electrical systems: a review," *International Journal of Dynamics and Control*, vol. 10, pp. 999-1011, Jan. 2022, doi: 10.1007/s40435-021-00892-3.
- [26] X. Guo, X. Yan, and K. Jermsittiparsert, "Using the modified mayfly algorithm for optimizing the component size and operation strategy of a high temperature PEMFC-powered CCHP," *Energy Reports*, vol. 7, pp. 1234-1245, Nov. 2021, doi: 10.1016/j.egy.2021.02.042.
- [27] S. Bazi, R. Benzid, Y. Bazi, and M. M. Al Rahhal, "A fast firefly algorithm for function optimization: application to the control of BLDC motor," *Sensors*, vol. 21, no. 16, p. 5267, Aug. 2021, doi: 10.3390/s21165267.
- [28] X.-S. Yang, "A new metaheuristic bat-inspired algorithm," in *Nature inspired cooperative strategies for optimization (NICSO 2010)*, vol. 284, pp 65-74, 2010, doi: 10.1007/978-3-642-12538-6\_6.
- [29] R. Ramachandran, J. S. Kumar, and B. Madasamy, "A hybrid MFO-GHNN tuned self-adaptive FOPID controller for ALFC of renewable energy integrated hybrid power system," *IET Renewable Power Generation*, vol. 15, no. 7, pp. 1582-1595, Mar. 2021.

## BIOGRAPHIES OF AUTHORS



**Ms. Sushita Kanagaraj**    did her BE degree from Goa University, Goa, India and ME Degree from PSG College of Technology, Anna University, Chennai, India. She is working as assistant professor in the Department of Electrical and Electronics Motorering, Vels Institute of Science, Technology & Advanced Studies (VISTAS), Tamilnadu, India. Her field of interest includes electric vehicle control and charging, neural networks and fuzzy logic control, motor drive, and power converter. She can be contacted at email: sushita.se@velsuniv.ac.in.



**Dr. Shanmugasundaram Nithaiyan**    received his BE in Electrical and Electronics Motorering from Anna University, Chennai, India. He did ME in Power Electronics and Industrial Drives from Sathyabama University, Chennai, India and PhD in Electrical Motorering from Anna University Chennai, Tamilnadu, India. He is working as an associate professor in the Department of Electrical and Electronics Motorering, Vels Institute of Science, Technology and Advanced Studies (VISTAS), Tamil Nadu, India. His field of interest includes electrical machines and control, electric vehicle control and charging, power converters and power cable modeling. He can be contacted at email: shanmugam71.se@velsuniv.ac.in.